Viscoelastic Relaxation and Molecular Mobility of Hyperbranched Poly(ϵ-caprolactone)s in Their Melt State

Seung-Yeop Kwak,*,† Jeongsoo Choi,‡ and Hee Jae Song‡

Hyperstructured Organic Materials Research Center (HOMRC), Research Institute of Advanced Materials (RIAM), and School of Materials Science and Engineering, Seoul National University, San 56-1, Shinlim-dong, Kwanak-ku, Seoul 151-744, Koreaa

Received August 6, 2004

The dynamic viscoelastic relaxation behavior and the molecular mobility of a series of hyperbranched poly(ϵ-caprolactone)s (HPCLs) possessing molecular architectural variation and their linear counterpart, linear poly(ϵ-caprolactone) (LPCL), were characterized and evaluated in conjunction with their specific molecular architectures which are the different lengths of the linear backbone segments and the different relative degrees of branching (DBs). The relative DBs, determined by the branching ratio values, were in decreasing order of HPCL-5 > HPCL-10 > HPCL-20. Dynamic viscoelastic relaxation measurements exhibited unentangled behavior for HPCLs compared to the apparently entangled linear, and the parallel $G'(\omega)$ and $G''(\omega)$ curves were observed for the HPCLs, while the LPCL exhibited a typical curve. The melt dynamics of HPCLs was observed to be complex. This characteristic dynamic behavior of HPCLs, particularly incorporating the shorter segments, can be seen to be another example of gellike power-law relaxation of hyperbranched systems. The correlation time, τ_c, was determined from the $G''(\omega)$ and the empirical Havriliak−Negami (HN) equation, which provided a unique means to evaluate the molecular mobility. Further insights to the correlation times with the Arrhenius equation provided novel information about the temperature-dependence of the molecular mobility and the activation energy, E_a. The molecular mobility of three HPCLs was found to be higher than that of LPCL, and was observed to enhance with decreasing lengths of oligo(ϵ-caprolactone) segments and increasing relative DB.

Introduction

Recently, viscoelastic relaxation behavior and molecular motion in polymers have received considerable attention as a bridge in making connections in the structure−property relationships since such aspects of molecular behavior are inevitably related to the chemical structure and molecular environment and which consequently exert the greatest influence on the relevant physical and mechanical properties in their end use.[1−6] Viscoelastic relaxation and molecular motions are related to the state of polymeric materials which changes according to the change in temperature. Neither chain diffusion nor segmental motion occur to any appreciable extent in the glassy region, whereas in the intermediate rubbery-plateau region segmental motion is possible but chain diffusion is very limited. Then, in the terminal flow region, both motions can be observed.[7] The close interdependence of the molecular relaxation and the constraints input suggests that our observation of the molecular motion varies to some degree in accordance with the measurement techniques used. Thus, it is noteworthy that various observations of the molecular motion can be quantitatively characterized by means of the term correlation time, τ_c, which is defined as the average relaxation time required for the motional events.[8] The correlation times usually fall within a range that typically covers 13 decades of time, $10^{-9} > \tau_c > 10^4$ sec, and have been measured for various polymeric materials by numerous techniques.[9] Among these techniques, nuclear magnetic resonance (NMR) relaxation, dielectric relaxation, and dynamic viscoelastic relaxation are the most widely used. NMR relaxation reflects the modulation events of magnetic dipoles, which are on a local scale and of a relatively low energy, and the τ_c is several orders of magnitude shorter than that from dielectric or dynamic viscoelastic relaxation.[5,10,11] Dielectric relaxation has also been used extensively because of its wide-frequency capabilities, but is limited to detecting only the motions of

* To whom correspondence should be addressed. Tel: +82-2-880-8365. Fax: +82-2-885-1748. E-mail: sykwak@snu.ac.kr.
† HOMRC and Seoul National University.
‡ RIAM and Seoul National University.

(1) Bailey, R. T.; North, A. M.; Pethrick, R. A. *Molecular Motion in High Polymers*; Oxford University Press: New York, 1981.
(2) North, A. M. In *Molecular Behavior and Development of Polymeric Materials*; Ledwith, A., North, A. M., Eds.; Chapman and Hall: London, 1975.
(3) North, A. M. In *Essays in Chemistry, Vol. 4*; Bradley, J. N., Hudson, R. F., Gillard, R. D., Eds.; Academic Press: London and New York, 1972.
(4) McCrum, N. G.; Read, B. E.; Williams, G. *Anelastic and Dielectric Effects in Polymeric Solids*; Wiley: New York, 1967.
(5) Kwak, S.-Y.; Lee, H. Y. *Macromolecules* **2000**, *33*, 5536.
(6) Kwak, S.-Y.; Ahn, D. U. *Macromolecules* **2000**, *33*, 7557.
(7) Ferry, J. D. *Viscoelastic Properties of Polymers*, 3rd ed.; Wiley: New York, 1980.
(8) McCall, D. W. *Acc. Chem. Res.* **1971**, *4* (6), 223.
(9) McBrierty, V. J.; Packer, K. J. *Nuclear Magnetic Resonance in Solid Polymers*; Cambridge University Press: Cambridge, U.K., 1993.
(10) Jones, A. A. In *High-Resolution NMR Spectroscopy of Synthetic Polymers in Bulk*; Komoroski, R. A., Ed.; VCH Publishers: Deerfield Beach, FL, 1986.
(11) Kulik, A. S.; Beckham, H. W.; Schmidt-Rohr, K.; Radloff, D.; Pawelzik, U.; Boeffel, D.; Spiess, H. W. *Macromolecules* **1994**, *27*, 4746.

10.1021/cm0487021 CCC: $30.25
Published on Web 02/04/2005

the electric dipole of the chemical bonds in the backbone.[12] Dynamic viscoelastic relaxation prevails over other techniques due to its useful aspect from the practical point of view.[6,7] Molecular motion and rheological behavior observed by this technique provide insights into the intermolecular interactions and the effects that molecular variables such as chemical nature and specific molecular architecture have on bulk properties.

Hyperbranched polymers (HBPs) have been increasingly considered as strong candidates for tailor-made materials with high performance and/or novel functionality at a reasonable cost due to the advantage of their synthetic simplicity along with their unique physical and chemical properties.[5,6,13−16] The most recently developed hyperbranched poly(ϵ-caprolactone)s (HPCLs) are considered to be one of the most attractive hyperbranched polymers, because when the synthetic approach is applied to this polymer, it produces a homologous series of HPCLs with a range of molecular architectural variation, i.e., linear backbone segments with differing lengths and different numbers of branching points.[17−19] Because of the close relationship between rheology and processing properties, the characterization of the rheological behavior of hyperbranched polymers is important for exploring their practical applicability.[20−22] Studies on rheological behavior of hyperbranched molecules were first initiated on hyperbranched and star-branched aliphatic polyesters in the mid-1990s by a group of researchers at the Royal Institute of Technology in Stockholm.[23−26] Although there have been some advances in the study of rheological behavior of perfect dendrimers since then,[27−30] study of those that are hyperbranched has been relatively lagging. And, to our knowledge, there have not yet been any studies conducted on the viscoelastic relaxation behavior of hyperbranched polymers with architectural variation and the effect of architectural variation on their rheological behavior and molecular mobility.

(12) Kremer, F.; Arndt, M. In *Dielectric Spectroscopy of Polymeric Materials*; Runt, J. P., Fitzgerald, J. J., Eds.; American Chemical Society: Washington, DC, 1997.
(13) Fréchet, J. M. J. *Science* **1994**, *263*, 1710.
(14) Webster, O. W. *Science* **1991**, *251*, 887.
(15) Newkome, G. R. *Advances in Dendritic Molecules*; JAI Press: Greenwich, CT, 1994; Vol. 1.
(16) Kim, Y. H.; Webster, O. W. *J. Am. Chem. Soc.* **1990**, *112*, 4592.
(17) Trollsås, M.; Hedrick, J. L.; Mecerreyes, D.; Dubois, Ph.; Jérôme, R.; Ihre, H.; Hult, A. *Macromolecules* **1997**, *30*, 8508.
(18) Trollsås, M.; Atthoff, B.; Claesson, H.; Hedrick, J. L. *Macromolecules* **1998**, *31*, 3439.
(19) Trollsås, M.; Hedrick, J. L. *Macromolecules* **1998**, *31*, 4390.
(20) Malmström, E.; Hult, A. *J. Macromol. Sci., Rev. Macromol. Chem. Phys.* **1997**, *C37*, 555.
(21) Voit, B. *J. Polym. Sci., Part A: Polym. Chem.* **2000**, *38*, 2505.
(22) Gao, C.; Yan, D. *Prog. Polym. Sci.* **2004**, *29*, 183.
(23) Johansson, M.; Malmström, E.; Hult, A. *J. Polym. Sci., Part A: Polym. Chem.* **1993**, *31*, 619.
(24) Malmström, E.; Johansson, M.; Hult, A. *Macromolecules* **1995**, *28*, 1698.
(25) Malmström, E.; Hult, A. *Macromolecules* **1996**, *29*, 1222.
(26) Malmström, E.; Hult, A.; Gedde, U. W.; Liu, F.; Boyd, R. H. *Polymer* **1997**, *38*, 4873.
(27) Hawker, C. J.; Farrington, P. J.; Mckay, M. E.; Wooley, K. L.; Fréchet, J. M. J. *J. Am. Chem. Soc.* **1995**, *117*, 4409.
(28) Farrington, P. J.; Hawker, C. J.; Fréchet, J. M. J.; Mckay, M. E. *Macromolecules* **1998**, *31*, 5043.
(29) Uppuluri, S.; Keinath, S. E.; Tomalia, D. A.; Dvornic, P. R. *Macromolecules* **1998**, *31*, 4498.
(30) Uppuluri, S.; Morrison, F. A.; Dvornic, P. R. *Macromolecules* **2000**, *33*, 2551.

In the present paper, hyperbranched poly(ϵ-caprolactone)s (HPCLs), designed to incorporate the different lengths of the linear homologous oligo(ϵ-caprolactone) backbone segments consisting of 5, 10, and 20 ϵ-caprolactone monomer units (thereby referred to as HPCL-5, -10, and -20, respectively), were synthesized, and their dynamic viscoelastic relaxation behavior and the molecular mobility were compared to those of their linear counterpart (LPCL) whose chemical structure are identical and molecular weights are similar to those of HPCLs. The relative degrees of branching (DBs) for the HPCLs were determined by the branching ratio values calculated from the ratio of mean-square radius of gyration of each HPCL to that of LPCL. The focal point of this study is to elucidate and compare the dynamic viscoelastic relaxation behavior and the molecular mobility of the HPCLs and the LPCL in their melt state in conjunction with the molecular architectural difference which is the different length of the linear backbone segments and the different relative DB.

Experimental Section

Materials. α-Carboxylic-ω-dihydroxy AB_2 macromonomers **3**, 2,2-bis[ω-hydroxyoligo(ϵ-caprolactone)methyl]propionic acids, in which the branching point is predefined and the reactive functionalities are less sterically hindered, were synthesized according to a reaction developed by Trollsås et al. (Scheme 1).[19]

The dihydroxy-functional initiator **1**, 2,2-bis-(hydroxymethyl)-propyl benzoate, was prepared by the esterification of 2,2-bis-(hydroxymethyl)propionic acid (bis-MPA) with benzyl bromide. Ring-opening polymerization of ϵ-caprolactone from **1** in the presence of a catalytic amount of tin(II) 2-ethylhexanoate ($Sn(Oct)_2$) produced benzyl-protected AB_2 macromonomers **2**, 2,2-bis[ω-hydroxyoligo(ϵ-caprolactone)methyl]propyl benzoates, with accurate control of the length of oligo(ϵ-caprolactone) segments and with narrow molecular weight distribution. The lengths of oligo(ϵ-caprolactone) segments incorporated in the final hyperbranched poly(ϵ-caprolactone)s (HPCLs) were defined in this step, where the targeted values were determined by the feed ratios of monomer-to-initiating hydroxyl group molar ratio ($[\epsilon\text{-CL}]_0/[-\text{OH}]_0$). The benzyl protecting group in **2** was readily removed by catalytic hydrogenolysis under hydrogen (H_2) atmosphere to give **3** capable of self-condensing polymerization. The novel AB_2 macromonomers obtained via this synthetic route were reported to give an inherently higher degree of branching in the resulting hyperbranched polymers due to the predefined and perfectly dendritic branching point. Finally, the HPCLs in this study were prepared by vacuum melt polycondensation of **3**. The mixture of **3** and *p*-toluenesulfonic acid (TSA) was allowed to react at 110 °C under a stream of argon, removing the water formed during the reaction. After 2 h, the argon stream was turned off, and the flask was sealed and connected to a vacuum line (10^{-2} Torr, cooling trap) for 3 h. Then, the mixture was dissolved in tetrahydrofuran (THF) and precipitated into methanol (MeOH) to give **4** as white solids. The ^{1}H NMR spectrum of HPCL-10 is shown in Figure 1 with the corresponding peak assignments. The difference in NMR spectra of HPCLs lies only in the ratio of the integral of repeating unit peak (δ 2.22, *d* in Figure 1) to that of chain-end peak (δ 3.59, *c* in Figure 1). The architectural verification shall be discussed in more detail in the Results and Discussion section. To investigate and compare the role of hyperbranched structure against conventional linear structure, linear poly(ϵ-caprolactone) (LPCL), whose chemical structure is identical and molecular weight is similar to those of HPCLs, was purchased

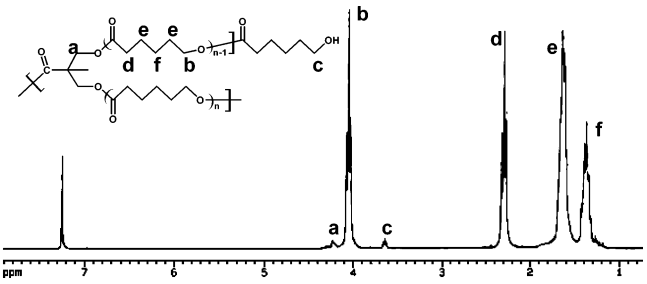

Figure 1. ^{1}H NMR spectrum (300 MHz) of HPCL-10.

Scheme 1. Syntheses of Hyperbranched Poly(ϵ-caprolactone)s

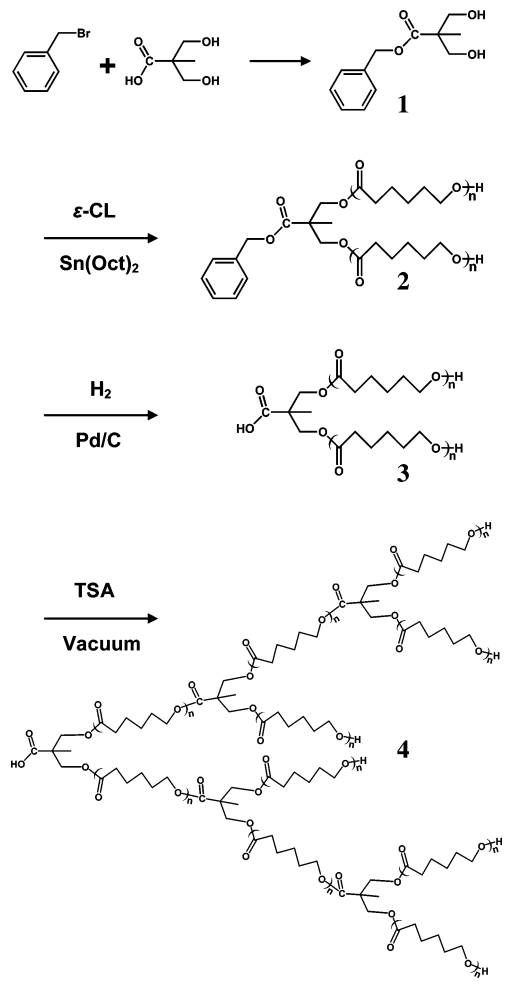

from Aldrich Chemical (M_n = 10 000; polydispersity index = 1.4) and used as a linear counterpart to HPCLs.

General Characterization. ^{1}H NMR spectra were obtained on a Bruker Avance DPX 300 (300 MHz for ^{1}H) spectrometer with the tetramethylsilane (TMS) proton signal as an internal standard in chloroform-*d*. A size-exclusion chromatograph (SEC) modular system consisted of a Dionex DG-1210 degasser, a Dionex P680 HPLC pump, a Dionex automatic sample injector, and a set of five size-exclusion columns (Ultra-micro Styragel, $10^5 \times 2$, 10^4, 10^3, 500 Å). A MiniDAWN (Wyatt Technology, Santa Barbara, CA) multi-angle laser light scattering (MALLS) detector equipped with a 690-nm semiconductor laser was installed between the size-exclusion columns and a Wyatt Optilab DSP differential refractometer. The calibration curves and the molecular weights distribution were computed by Astra software (Version 4.90.04). The calibration of detectors was achieved using polystyrene standards of narrow molecular weights distribution and known molecular weights. The differential refractive index increment (dn/dc) in a mixed solvent (THF/DMF, 10/1, v/v; and $LiNO_3$ 2 g/L) at 25 °C was determined for poly(ϵ-caprolactone) with a Wyatt Optilab DSP interferometric differential refractometer, operated at 690 nm and calibrated with aqueous NaCl solutions. The radii of gyration (R_g) of three HPCLs and an LPCL were measured by small-angle X-ray scattering (SAXS) and the SAXS intensity distribution $I(q)$ was measured with a rotating-anode X-ray generator (Bruker AXS Nanostar) operated at 40 kV and 35 mA. The X-ray source was monochromatized Cu Kα (λ = 1.54 Å) radiation, and the scattering angle range was 0.5−2.5°. The melting temperatures, T_m, of three HPCLs and an LPCL were determined by differential scanning calorimetry (DSC) with a TA instruments DSC 2920 at heating rates of 10 °C/min under a nitrogen atmosphere.

Frequency-Sweep Dynamic Viscoelastic Relaxation Measurements. The dynamic viscoelastic relaxation properties of three HPCLs and an LPCL were measured with a Paar Physica UDS-200 mechanical spectrometer. The measurements were performed in dynamic shear oscillatory mode using 25-mm-diameter parallel disk geometry with a gap setting of ca. 2 mm. The angular frequency ranged from 0.1 to 100 rad/s and the temperature was set to between 55 and 175 °C for the three HPCLs, and 60 and 180 °C for the LPCL with an increasing interval of 20 °C. Individual samples were tested with parallel-plate geometry isothermally under a thermally regulated nitrogen atmosphere. The lowest temperature of the measurements was restricted to be above the melting temperature, i.e., $T_m + 5 \sim 10$ °C, depending on the samples, so as to prevent slippage between the sample and the disk from occurring. The strain amplitude of 20% was selected to be large enough for accurate torque signals but small enough to keep the material response in the linear region. The linear viscoelastic (LVE) region was determined by dynamic strain sweep tests.

Results and Discussion

Synthesis and General Characterization. The AB_2 macromonomers **3** and the hyperbranched poly(ϵ-caprolactone)s (HPCLs) **4** were synthesized according to a reaction first developed by Trollsås et al.[19] and were recently modified in our previous study, in which the HPCLs were successfully prepared by polycondensation with continuous removal of water in a less moisture-sensitive reaction condition[31] (Scheme 1). The AB_2 macromonomers were prepared to incorporate three different lengths of homologous oligo(ϵ-caprolactone) segments by ring-opening polymerization with variable ϵ-caprolactone-to-initiating hydroxyl group molar ratio ($[\epsilon\text{-CL}]_0/[-\text{OH}]_0$ = 5, 10, and 20, respectively) followed by hydrogenolysis deprotection, which explains the names given as AB_2-5, -10, and -20, respectively. Thus, the HPCLs were prepared to have intrinsically different lengths of backbone segments by the use of the different AB_2 macromonomers, referred to respectively as HPCL-5, -10, and -20. Listed in Table 1 are the general characteristics of three HPCLs and their linear counterpart, LPCL.

The average number of ϵ-caprolactone monomer units incorporated in the AB_2 macromonomers $\langle N_{\epsilon-CL}\rangle$, which are the lengths of homologous oligo(ϵ-caprolactone) segments in the final HPCLs, was calculated from the ratios of the integrated area of the peak corresponding to the repeating methylene units ($-COCH_2$, δ 2.22, Figure 1 d) to the

(31) Choi, J.; Kwak, S.-Y. *Macromolecules* **2003**, *36*, 8630.

Table 1. General Characteristics of Hyperbranched Poly(ϵ-caprolactone)s and Their Linear Counterpart

	AB_2 macromonomers						
sample	entry[a]	$[\epsilon-CL]_0/[-OH]_0$[b]	$\langle N_{\epsilon-CL}\rangle$[c]	$\langle N_{AB2}\rangle$[d]	$M_{n,NMR}$[e]	M_n[f]	M_w/M_n[f]
HPCL-5	AB_2-5	5	5.7	8.1	11 510	11 800	1.8
HPCL-10	AB_2-10	10	10.3	5.1	12 700	12 600	1.6
HPCL-20	AB_2-20	20	20.1	3.3	15 100	15 700	1.5
LPCL[g]						10 700	1.4

[a] AB_2 macromonomers used for the preparation of hyperbranched poly(ϵ-caprolactone)s. [b] ϵ-Caprolactone monomer-to-initiating hydroxyl group molar ratio. [c] Average number of ϵ-caprolactone units incorporated in the AB_2 macromonomers determined by ^{1}H NMR. [d] Average number of the AB_2 macromonomer units incorporated in the HPCLs determined by ^{1}H NMR. [e] Number average molecular weights determined by ^{1}H NMR. [f] Obtained from SEC-MALLS. [g] Linear poly(ϵ-caprolactone) (Aldrich Chemical).

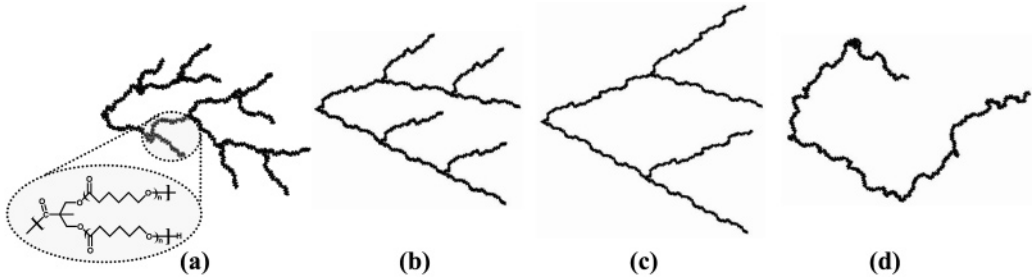

Figure 2. Schematic drawings of (a) HPCL-5, (b) HPCL-10, (c) HPCL-20, and (d) LPCL. The inset in (a) represents the AB_2 macromonomer units incorporated in the HPCLs.

integrated area of the peak corresponding to the chain ends ($-CH_2OH$, δ 3.59, Figure 1 c) in ^{1}H NMR spectra of the AB_2 macromonomers. The calculated $\langle N_{\epsilon-CL}\rangle$ values were in close agreement with the targeted values solely predictable from $[\epsilon\text{-CL}]_0/[-OH]_0$. (Table 1) In a similar manner, the average number of AB_2 macromonomer units incorporated in the HPCLs $\langle N_{AB2}\rangle$ was calculated from the following equation based on the branching theories developed by Flory:[32] $\langle N_{AB2}\rangle = m/\{2\langle N_{\epsilon-CL}\rangle - m\}$ with m being the ratios of the integrated area of the peak corresponding to the repeating methylene units to the integrated area of the peak corresponding to the chain ends of the HPCLs. The calculated $\langle N_{AB2}\rangle$ values were decreased with increasing the lengths of linear segments in the AB_2 macromonomers that might be caused by the increase in the steric hindrance and the decrease in the number of functional sites in unit volume.

Molecular architectural variation among the HPCLs and the LPCL in this study is well reflected in Figure 2, which shows schematic drawings of the HPCL molecules and the LPCL molecule. The average length of oligo(ϵ-caprolactone) segments and the average number of macromonomers in hyperbranched molecules were determined to be $\langle N_{\epsilon-CL}\rangle$ and $\langle N_{AB2}\rangle$, respectively, on the assumption that the reactivity of B parts in the AB_2 macromonomers are equal, and thus macromonomers were randomly incorporated.

Size exclusion chromatography (SEC) with a multi-angle laser light scattering (MALLS) detector was used to determine molecular weights and molecular weight distributions of three HPCLs. It is generally considered that hyperbranched polymers give inaccurately low molecular weight characterization during conventional SEC analysis, which is based on the linear standards, due to the decreased hydrodynamic volume imposed by branching.[33] However, molecular weight data obtained from SEC-MALLS were confirmed to be near absolute values through comparison with the values calculated from ^{1}H NMR end-group analyses (Table 1). As can be seen in Table 1, the molecular weights are not significantly varied among the HPCLs and are also similar to that of the LPCL.

Another important material characteristic with which the molecular architectures of hyperbranched polymers can be described is the degree of branching (DB), which is commonly determined by the relative proportions among the NMR resonance peak areas pertinent to the respective dendritic, linear, and terminal units of the given hyperbranched polymer whenever there exist distinguishable corresponding chemical shifts. Unfortunately, the HPCLs in this study did not show any such distinguishable ^{1}H resonance peaks that would have been useful for calculating DB and lacked quaternary carbons unique for determining DB. Therefore, the information about DB of the HPCLs were alternatively characterized through the comparison of the molecular dimensions of hyperbranched molecules against their linear counterpart, taking into consideration the fact that as more highly branched structures are imparted, the molecular dimensions get decreased. The information about DB obtained in this way is a relative value. It is noteworthy that the branching ratio, g, which is the ratio of mean-square radius of gyration of a given hyperbranched polymer to that of its linear counterpart of the same chemical structure and the analogous molecular weights, provides an alternative means to characterize the branching structure and hence obtain information about relative DB:[34]

$$g = \frac{\langle R_g^2\rangle_{branched}}{\langle R_g^2\rangle_{linear}} \quad (1)$$

The parameter g is always less than 1 and decreases with the increase in DB because the branched molecules become more compact compared with the less branched molecules

(32) Flory, P. J. *J. Am. Chem. Soc.* **1952**, *75*, 2718.
(33) Zimm, B. H.; Stockmayer, W. H. *J. Chem. Phys.* **1949**, *17*, 1301.
(34) Podzimek, S. *J. Appl. Polym. Sci.* **1994**, *54*, 91.

Table 2. Radius of Gyration, Branching Ratio, and Melting Temperature of Hyperbranched Poly(ϵ-caprolactone)s and Their Linear Counterpart

sample	R_g (nm)[a]	g[b]	T_m (°C)[c]
HPCL-5	4.57	0.76	44
HPCL-10	4.77	0.83	49
HPCL-20	5.18	0.98	52
LPCL	5.23	1	57

[a] Determined from SAXS curves fit by Zimm scattering function. [b] Branching ratio. [c] Melting temperatures observed on second heating.

or the corresponding linear counterpart of similar molecular weight. The root-mean-square radii $\langle R^2\rangle^{1/2}$ (equivalently called radii of gyration R_g) of three HPCLs and an LPCL were determined by SAXS by performing weighted nonlinear, least-squares fits to the scattering curves over the accessible q range with the Zimm particle scattering function, $P_{Zimm}(R_g,q)=1/[1 + q^2R_g^2/3]$, which was reported to be the most suitable for determining R_g for hyperbranched polymers.[35] Listed in Table 2 are the radii of gyration for all HPCLs and an LPCL and calculated values of branching ratio. Taking into consideration the fact that the relative DB increases with the decrease in branching ratio, it is concluded that the relative DB increased in the order of HPCL-20 < HPCL-10 < HPCL-5, indicating that the relative DB increased with the decrease in the length of linear oligo(ϵ-caprolactone) segments in the HPCLs. Specific molecular architectural changes by incorporating branching structure have been investigated on other branched polymers such as star and comblike polymers as well as hyperbranched polymers.[36−40] For example, Roovers determined branching ratios of some comb polystyrenes from the ratios of radii of gyration of combs which are experimentally measured against those of their linear counterpart which are theoretically calculated.[36,37] Determined branching ratios ranged from 0.25 to 0.89 for comb polystyrenes all having approximately 30 branches. It is also found in the Roovers' work that the branching ratios for combs having a longer chain with the similar number of branches increased compared to those having shorter chain. This confirms that the smaller branching ratio of HPCL-5, in comparison to those of the HPCL-10 and -20, is mainly the result of the larger number of branches of HPCL-5. This observation has also been reported in the work of Vlassopoulos et al., where it was demostrated that multiarm star polymers having larger numbers of arms resulted in smaller radii of gyration compared to that of stars having a smaller number of arms with almost the same molecular weight.[38] A densely packed structure resulting from the highly branched topology in hyperbranched polymers has been sometimes characterized by contraction factors, $g' = [\eta]_{branched}/[\eta]_{linear}$.[4,5] Estimated values of contraction factors ranged from 0.2 to 0.8, and decreased for more highly branched molecules. However, it is noteworthy that contraction factors are different from branching ratios, and the relation between these two quantities is often expressed in terms of the exponent ϵ as $g' = g^{\epsilon}$.[36,39,40] Therefore, contraction factors for hyperbranched polymers in the literature could not be directly compared to branching ratios in this study. Details on the determination of branching ratios of HPCLs have already been reported in our previous study.[31]

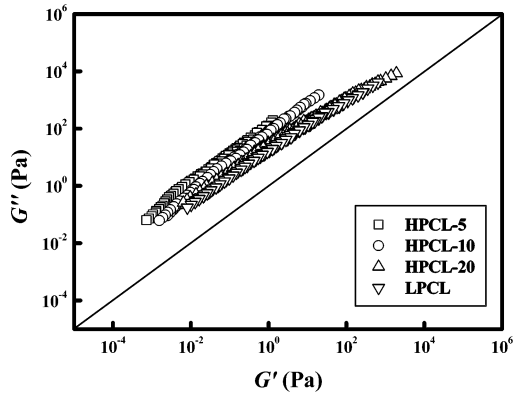

Figure 3. Logarithmic plots of the shear loss modulus $G''(\omega)$ versus the shear storage modulus $G'(\omega)$ for HPCL-5 (□), HPCL-10 (○), HPCL-20 (△), and LPCL (▽) at various temperatures.

Differential scanning calorimetry (DSC) was used to characterize the melting temperatures (T_m) of three HPCLs and an LPCL, which are listed in Table 2. Shorter branches, brought about by the use of the AB_2 macromonomers with shorter linear segments and affected by the increase in relative DB, are assumed to have probably caused the decrease in T_m values in the order of HPCL-5 < HPCL-10 < HPCL-20 < LPCL.

Dynamic Viscoelastic Relaxation Behavior. Figure 3 shows the logarithmic plots of the shear loss modulus, $G''(\omega)$, versus the shear storage modulus, $G'(\omega)$, both taken at the same frequency ω for three HPCLs and an LPCL at various experimental temperatures.

In general, the $G''(\omega)$ versus $G'(\omega)$ plots have been used for investigating the effects of temperature, molecular weight and its distribution, branching architecture, and the phase structure of the polymers on the viscoelastic behavior of bulk polymers. In previous studies, it was reported that the $G''(\omega)$ versus $G'(\omega)$ curves shifted to the $G'(\omega)$ region as the molecular weight, the molecular weight distribution, and/or the length of branching were increased.[41−45] Another merit of the $G''(\omega)$ versus $G'(\omega)$ plot is that it provides a critical examination of the applicability of the superposition principle with respect to time−temperature correspondence. In the linear viscoelastic region, assuming that no changes are made to the structure within the assumed temperature range, the $G''(\omega)$ or $G'(\omega)$ versus ω plots at different temperatures can be superimposed to form a master curve. In Figure 3, the $G''(\omega)$ versus $G'(\omega)$ curves of three HPCLs and an LPCL

(35) Prosa, T. J.; Bauer, B. J.; Amis, E. J.; Tomalia, D. A.; Scherrenberg, R. *J. Polym. Sci., Part B: Polym. Phys.* **1997**, *35*, 2913.
(36) Roovers, J. *Polymer* **1979**, *20*, 843.
(37) Roovers, J.; Graessley, W. W. *Macromolecules* **1981**, *14*, 766.
(38) Vlassopoulos, D.; Fytas, G.; Pakula, T.; Roovers, J. *J. Phys.: Condens. Matter* **2001**, *13*, R855.
(39) Simon, P. F. W.; Müller, A. H. E.; Pakula, T. *Macromolecules* **2001**, *34*, 1677.
(40) Robertson, C. G.; Roland, C. M.; Paulo, C.; Puskas, J. E. *J. Rheol.* **2001**, *45*, 759.
(41) Nakajima, N.; Harrell, E. R. In *Current Topics in Polymer Science Vol. III*; Ottenbrite, R. M., Utracki, L. A., Inoue, S., Eds.; Hanser: New York, 1987.
(42) Han, C. D.; Kim, J. K. *Macromolecules* **1989**, *22*, 1914.
(43) Han, C. D.; Chuang, H. K. *J. Appl. Polym. Sci.* **1985**, *30*, 2431.
(44) Han, C. D.; Jhon, M. S. *J. Appl. Polym. Sci.* **1986**, *32*, 3809.
(45) Han, C. D.; Kim, J. K. *Macromolecules* **1989**, *22*, 4292.

are positioned at the upper-left side of the figure, showing viscous response-dominant features for all samples. In addition, it can be seen that the curves in the case of HPCL-5 and HPCL-10 shifted to the $G''(\omega)$ region in contrast with that of the LPCL. Recognizing that the molecular weights and molecular weight distributions of HPCL-5, HPCL-10, and LPCL were not significantly varied, the deviation of the $G''(\omega)$ versus $G'(\omega)$ curves of HPCL-5 and HPCL-10 is assumed to be the result of the different branching architectures. These shifts in the curves toward the $G''(\omega)$ region can be ascribed to the short length of oligo(ϵ-caprolactone) segments incorporated in the AB_2 macromonomers, which are the branches in the final HPCLs used for the syntheses of HPCL-5 and HPCL-10. Moreover, the higher relative DBs of HPCL-5 and HPCL-10 can be deduced to cause the shortening of the branches. However, the $G''(\omega)$ versus $G'(\omega)$ curve of HPCL-20 was positioned at almost the same region as that of the LPCL, which can be explained by the fact that (1) only a little branching was imposed in the molecules as shown in the value of branching ratio near that of the LPCL, and (2) a slightly higher molecular weight of HPCL-20 might offset the effect of branching on the shortening of branches. On the basis of the foregoing, we concluded that the order of length of oligo(ϵ-caprolactone) segments incorporated in the AB_2 macromonomers and the relative DB of the HPCLs is reflected by the order of shifts of the $G''(\omega)$ versus $G'(\omega)$ curves toward $G''(\omega)$ region.

It is noteworthy that the $G''(\omega)$ versus $G'(\omega)$ data for all HPCLs and the LPCL at varying temperatures fall on one curve as shown in Figure 3, which means that the time−temperature superposition principle could be applied to each HPCL and the LPCL, and further, the $G''(\omega)$ versus $G'(\omega)$ curves could be shifted along the frequency axis to form master curves. The results for a case in which the time−temperature superposition principle was applied are shown in Figure 4 in the form of moduli versus reduced frequency ($a_T\omega$) for HPCL-5, -10, and -20, and LPCL, respectively. Here, the moduli data were shifted vertically for clarity and corresponding scales can be found at the end of each arrow.

The vertical shift for construction of master curves was assumed to be negligible, and the same horizontal shift factor, a_T, was used for shifting both $G'(\omega)$ and $G''(\omega)$ along the frequency axis with respect to the reference curve at 115 °C for HPCLs and at 120 °C for LPCL. From Figure 4, it is clear that the data for HPCLs indicate features of unentangled behavior of the hyperbranched polymer compared to the apparently entangled linear. In addition, it can be seen that the linear data barely reached the $G''(\omega)$, $G'(\omega)$ terminal crossover at high frequencies when the moduli values were extended for about an additional 5 decades. This is well explained by the molecular weight of the LPCL being near the range of entanglement molecular weight, M_e, which was reported to be about 15 000−16 000 for linear poly(ϵ-caprolactone) in the literature.[46] At the same time, the moduli data of the HPCLs which are expected to have the same entanglement molecular weight due to the same chemistry, do not even show any crossover tendency with the same

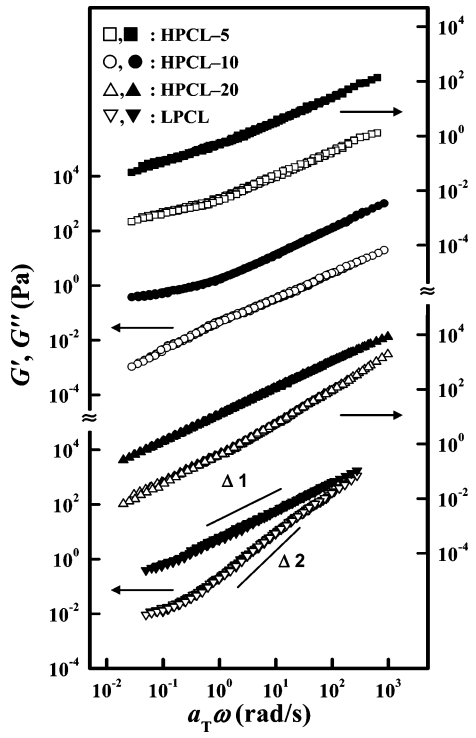

Figure 4. Master curves of the dynamic moduli $G'(\omega)$ (open symbols) and $G''(\omega)$ (filled symbols) for HPCL-5 (□,■), HPCL-10 (○,●), HPCL-20 (△,▲), and LPCL (▽,▼), representing the behavior over an extended frequency scale (T_0 = 115 °C for HPCLs and 120 °C for LPCL). The moduli data were shifted vertically for clarity.

extension of moduli of 5 decades. This is another example of unentangled behavior of hyperbranched polymer except that HPCLs in this study incorporate quite long linear branches in the backbones. Average molecular weights of independent branches of each HPCL range from 1000 to 3400, showing that molecular weights of linear branches do not exceed M_e. The dynamic moduli spectra of HPCLs shown in Figure 3 are obviously deviated from Rouse of Zimm behavior. $G'(\omega)$ remains below $G''(\omega)$ for the range of frequency, and $G'(\omega)$ and $G''(\omega)$ of the HPCLs, especially of the HPCL-5 and HPCL-10, rise in an almost parallel fashion for the period of more than a decade. It should be noted that the Rouse-Zimm type of dynamic model tends to exhibit a high-frequency response whereby both $G'(\omega)$ and $G''(\omega)$ rise in a parallel fashion according to $\sim\omega^n$ with n being exponent.[47] So, the Rouse model rises with $\omega^{1/2}$ while the Zimm model rises with $\omega^{2/3}$. In this study, the estimated values of exponents for dynamic moduli $G'(\omega)$ and $G''(\omega)$ were 0.88 for HPCL-5 and 0.98 for HPCL-10 with the difference between the two moduli being less than 0.01. However, the corresponding exponents of HPCL-20 are 1.23 for $G'(\omega)$ and 0.91 for $G''(\omega)$, which seems to be intermediate between hyperbranched and linear system. Recently, Dorgan et al. reported that dynamic moduli of dendritically branched polystyrene rise in a parallel fashion for a period of more than a decade with the power-law exponents ranging from 0.75 to 0.48.[47] Also, García-Franco et al. reported the gellike behavior of a polymer having long chain branching, in which the increase in branching of a polymer resulted in decreased

(46) Grosvenor, M. P.; Staniforth, J. N. *Int. J. Pharm.* **1996**, *135*, 103.

(47) Dorgan, J. R.; Knauss, D. M.; Al-Muallem, H. A.; Huang, T.; Vlassopoulos, D. *Macromolecules* **2003**, *36*, 380.

values of exponents.[48] Seeing the similarity in both molecular architectures and rheological features with the previous contributions, the characteristic dynamic behavior of HPCLs of the present study is believed to be another example of gellike power-law relaxation of hyperbranched systems.

Also found were that the slopes of the logarithmic plots of $G'(\omega)$ versus ω and $G''(\omega)$ versus ω for the LPCL, as shown in Figure 4, had values near 2 and 1, respectively, which are in good agreement with the recognized fact that $G'(\omega)$ is proportional to ω^2 and $G''(\omega)$ is proportional to ω in their terminal flow region.[44,45] On the other hand, none of the HPCLs reached the terminal slope region, and HPCL-5 and HPCL-10 did not show any forward tendency toward the terminal flow regime. This terminal behavior has been previously reported for the linear viscoelastic responses of a family of branched molecules such as ω-functionalized three-arm star polymers,[49] multi-arm star polymers,[50] and comb polymers.[51] Vlassopoulos et al. reported that the viscoelastic response of multi-functional star polymers is characterized by the presence of a slow relaxation process which essentially relates to the dense impenetrable cores. Similarly, the viscoelastic response of the HPCLs at low frequency not reaching a terminal slope is believed to relate to the exponentially slow terminal relaxation of the inner branches. In addition, a low-frequency upturn beyond the slope of moduli data, as observed in Figure 4, may be the slow secondary relaxation mode due to the different molecular mechanism. This low-frequency relaxation has been reported to be associated with the overall particle movement in highly functionalized stars[50] as well as in hyperbranched molecules.[47] However, it could be possible that the phenomena may be alternatively attributable to the experimental artifacts associated with phase angle resolution; all measurements in the present study were performed within the instrumental range reported by the manufacturer, and at least more than 3 independent measurements resulted in the same moduli data for each sample.

Average Relaxation Time and Apparent Activation Energy. Dynamic shear moduli of three HPCLs and an LPCL as a function of temperature can be used to obtain a quantitative measure of their corresponding molecular motion. It is well-known that the relaxation behavior of a polymer system can be observed following an exponential relaxing process that occurs not within a single relaxation time but over a distribution of several relaxation times.[52] Thus, the dynamic mechanical data must be treated with empirical fitting functions to represent the relaxation behavior and to determine the single average relaxation times. To describe the frequency dependency of dynamic moduli analytically, the Havriliak−Negami (HN) equation was employed as a fitting function in this study. This HN equation

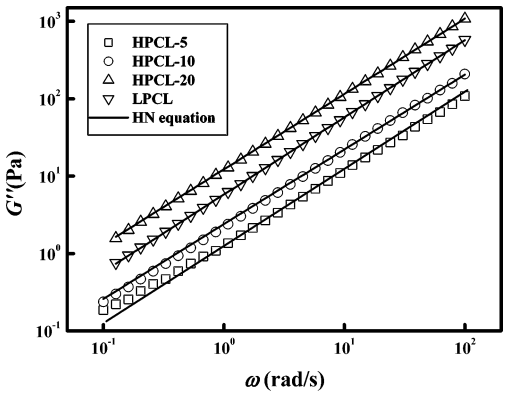

Figure 5. $G''(\omega)$ for HPCL-5 (□), HPCL-10 (○), HPCL-20 (△), and LPCL (▽) as a function of angular frequency at 115 °C for HPCLs and 120 °C for LPCL. The solid lines are the fits to the imaginary part of HN equation (eq 4).

was originally derived to fit the dielectric relaxation data but also can be used to analyze the dynamic mechanical relaxation data by appropriately changing the variables from the dielectric to the dynamic mechanical, assuming that the general relationships between them have already been determined.[53−56] The HN equation is given by

$$G^* = G' + iG'' = G_\infty + \frac{(G_0 - G_\infty)}{[1 + (i\omega\tau_{HN})^\alpha]^\gamma} \qquad (2)$$

with $0 < \alpha, \gamma < 1$ where α is a parameter characterizing a symmetric broadening of the distribution of relaxation times and γ characterizes an asymmetrical broadening. G^* is the complex shear modulus, G_0 and G_∞ are, respectively, the relaxed and unrelaxed modulus that can be estimated from the values of G' at low- and high-frequency, and τ_{HN} is the characteristic relaxation time. After the numerical evaluation of eq 2, considering an imaginary part of G^*, the storage and loss modulus may be derived as[57]

$$G'(\omega) = G_\infty + (G_0 - G_\infty) \times \frac{\cos(\gamma\theta)}{[1 + 2(\omega\tau_{HN})^\alpha\cos(\alpha\pi/2) + (\omega\tau_{HN})^{2\alpha}]^{\gamma/2}} \qquad (3)$$

$$G''(\omega) = (G_\infty - G_0) \times \frac{\sin(\gamma\theta)}{[1 + 2(\omega\tau_{HN})^\alpha\cos(\alpha\pi/2) + (\omega\tau_{HN})^{2\alpha}]^{\gamma/2}} \qquad (4)$$

with

$$\theta = \tan^{-1}\frac{(\omega\tau_{HN})^\alpha\sin(\alpha\pi/2)}{1 + (\omega\tau_{HN})^\alpha\cos(\alpha\pi/2)} \qquad (5)$$

The $G''(\omega)$ data (symbols) of three HPCLs and an LPCL are shown to fit well by HN equation (solid lines) as shown in Figure 5. It can be seen that $G''(\omega)$ of the samples at their

(48) García-Franco, C.; Srinivas, S. Lohse, D. J.; Brant, P. *Macromolecules* **2001**, *34*, 3115.
(49) Vlassopoulos, D.; Pitsikalis, M.; Hadjichristidis, N. *Macromolecules* **2000**, *33*, 9740.
(50) Kapnistos, M.; Semenov, A. N.; Vlassopoulos, D.; Roovers, J. *J. Chem. Phys.* **1999**, *111*, 1753.
(51) Daniels, D. R.; McLeish, T. C. B.; Crosby, B. J.; Young, R. N.; Fernyhough, C. M. *Macromolecules* **2001**, *34*, 7025.
(52) Matsuoka, S.; Quan, X. *Relaxation Phenomena in Polymers*; Oxford University Press: New York, 1992.
(53) Havriliak, S.; Negami, S. *Polymer* **1967**, *8*, 161.
(54) Lane, J. W.; Seferis, J. C. *Polym. Eng. Sci.* **1986**, *26*, 346.
(55) Nass, K. A.; Seferis, J. C. *Polym. Eng. Sci.* **1989**, *29*, 315.
(56) Boyd, R. H. *Macromolecules* **1984**, *17*, 903.
(57) Havriliak, S., Jr.; Havriliak, S. J. In *Dielectric Spectroscopy of Polymeric Materials*; Runt, J. P., Fitzgerald, J. J., Eds.; American Chemical Society: Washington, DC, 1997.

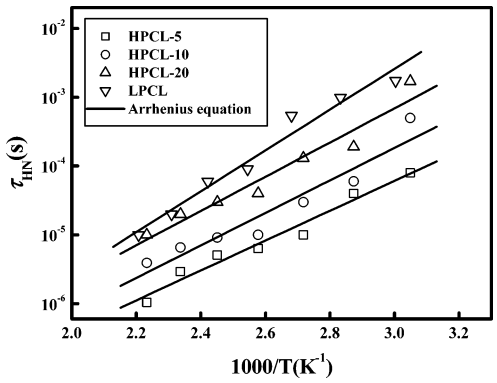

Figure 6. Correlation times, τ_c, for HPCL-5 (□), HPCL-10 (○), HPCL-20 (△), and LPCL (▽) as a function of temperature. The solid lines denote the fits to the Arrhenius equation (eq 6).

reference temperatures (115 °C for HPCLs and 120 °C for LPCL) is illustrated with their corresponding HN fitting results. The fitting is accomplished utilizing a specialized script running under the Origin software (version 6.0) from Microcal Software Inc. This script calls the Levenburg−Marquet minimization routine to provide the best fit parameters compared to the data sets. The procedure of the calculations is to fit the data to the $G''(\omega)$ data with eq 4 and then create the $G'(\omega)$ curve utilizing the set of fitted parameter values to evaluate the fitting results. As shown in Figure 5, the $G''(\omega)$ data of HPCLs and LPCL were found to fit well by the HN equation. Although not shown here, the fits to the $G'(\omega)$ data were found to maintain a good quality.

The correlation time, τ_c, which is the single average relaxation time, can be determined from the characteristic relaxation time, which is an adjusted parameter in the HN fitting equation, to be $\tau_c = \tau_{HN}$. The correlation times of three HPCLs and an LPCL as a function of temperature are shown in Figure 6. Throughout the entire range of experimental temperatures, all of the HPCLs exhibited shorter τ_c values than those of the LPCL, indicating the HPCLs possess faster molecular motion than that of their linear counterpart. Moreover, among the three HPCLs, as the length of oligo(ϵ-caprolactone) segments decreased and as the relative DB increased, the τ_c values decreased, hence causing the molecular motion to become faster.

Further insights into Figure 6 by fitting the τ_c values to the following Arrhenius equation provided novel information on the temperature dependence of the molecular motion and the apparent activation energy, $E_{a,\tau c}$, of each HPCL and the LPCL. The Arrhenius equation is expressed by

$$\tau_c = \tau_{c,0} \exp\left(\frac{E_a}{RT}\right) \quad (6)$$

where $\tau_{c,0}$ and R are the preexponential factor and the gas constant, respectively. As shown in Table 3, the apparent activation energies increase in the order of HPCL-5 < HPCL-10 < HPCL-20 < LPCL. Recognizing that the apparent activation energy corresponds to the barrier height for the potential hindering motion, the molecular mobility of three HPCLs was higher than that of their linear counterpart. In addition, the molecular mobility of each HPCL was enhanced by shortening the length of oligo(ϵ-caprolactone) segments and increasing the relative DB, which are in good agreement with the τ_c results. This can be explained by the fact that the higher relative DB caused the branches in the final HPCLs to become shorter, and intrinsically shorter branches were incorporated in the final HPCLs by using the AB_2 macromonomers having shorter oligo(ϵ-caprolactone) segments. Therefore, molecular motion in three HPCLs was generated more easily with the lower activation energy due to the existence of much shorter mobile branches, which were comparable to the LPCL that did not possess such branched structure. This behavior of the HPCLs approaches that of dendrimers as previously reported by Dvornic et al.[29,30] They reported that the architecturally unique dendrimer molecules exhibited Newtonian flow behavior and the absence of interdendrimer interaction, which set dendrimers apart from the conventional polymers with linear architecture.[29,30] HPCLs of the present study that exhibit unentangled behavior as well as the reduction of molecular mobility with the increase in the relative DB would set them as imperfectly branched analogues of dendrimers from the viewpoint of rheology.

Table 3. Correlation Time and Apparent Activation Energy for Hyperbranched Poly(ϵ-caprolactone)s and Their Linear Counterpart

sample	τ_c (sec)[a]	E_a (kJ/mol)[b]
HPCL-5	6×10^{-6}	41.5
HPCL-10	1×10^{-5}	45.3
HPCL-20	4×10^{-5}	47.6
LPCL	9×10^{-5}	56.8

[a] Measured at reference temperature. [b] Provided by fitting of correlation times with Arrhenius equation.

Conclusions

In the present paper, three hyperbranched poly(ϵ-caprolactone)s (HPCL-5, HPCL-10, HPCL-20) were prepared with structural variation in the backbone chains, which is the different lengths of homologous oligo(ϵ-caprolactone) segments and hence the different degree of branching (DB), through moisture-sensitive catalyst-free vacuum polycondensation. Also, dynamic viscoelastic relaxation behavior and molecular mobility of these HPCLs and their linear counterpart, LPCL, were characterized and interpreted in conjunction with their architectural characteristics.

(1) The molecular weights of the resulting HPCLs, which were determined by size exclusion chromatography connected to a multi-angle laser light scattering detector (SEC-MALLS) and confirmed by end-group analysis on ^{1}H NMR spectra, were not significantly varied. The ratio of mean-square radius of gyration of each HPCL to that of the LPCL, referred to as branching ratio, resulted in the relative degree of branching for individual HPCL, which was found to be considerably influenced by the length of linear oligo(ϵ-caprolactone) segments; the shorter the oligo(ϵ-caprolactone) segments, the higher the relative degree of branching in the order HPCL-5 > HPCL-10 > HPCL-20. In addition, correlative effect of DB on the thermal transition was also observed. The melting transition temperatures of the HPCLs were elevated in accordance with the increase in the length of oligo(ϵ-caprolactone) segments and hence decreasing the DB.

(2) From the loss shear modulus, $G''(\omega)$, versus storage shear modulus, $G'(\omega)$, curves of the HPCLs, it was predicted that the time−temperature superposition principle was applicable for the HPCLs and the LPCL considering that the moduli data measured at different temperatures fell on one curve. In the case of the HPCL-5 and the HPCL-10, the shifts of the $G''(\omega)$ versus $G'(\omega)$ curves from the reference curve of LPCL toward $G''(\omega)$ region were observed, which can be explained by (a) the intrinsically short oligo(ϵ-caprolactone) branches and (b) the shortening of branches with the increase in relative DB. However, the $G''(\omega)$ versus $G'(\omega)$ curve of the HPCL-20 was positioned at almost the same region to that of LPCL, which can be explained by the fact that (a) only a little branching was imposed in the molecules and (b) a slightly higher molecular weight of the HPCL-20 might offset the effect of branching on the shortening of branches.

(3) The master curves, where three HPCLs and an LPCL exhibited the $G''(\omega)$ over $G'(\omega)$ with an increase in both $G'(\omega)$ and $G''(\omega)$ along the shear rate within the experimental temperature range, indicating terminal flow behavior of unentangled polymers. However, none of the HPCLs reached a terminal slope region, and even HPCL-5 and HPCL-10 showed no tendency toward the terminal flow regime, while LPCL did. This phenomenon is believed to be related with the secondary slow terminal relaxation of the inner branches as reported in previous studies. In addition, it was also found that $G'(\omega)$ and $G''(\omega)$ of HPCLs, especially for HPCL-5 and HPCL-10, rise in a parallel fashion in accordance with $\sim\omega^n$ with n being 0.88 and 0.98, respectively. This confirms the fact that gellike power-law relaxation of hyperbranched system can be observed for the HPCLs with shorter segments and higher DB.

(4) The correlation time, τ_c, providing a unique means to evaluate the molecular mobility, was determined by utilizing the empirical Havriliak−Negami (HN) equation. The results showed that the molecular mobility of the HPCLs was higher than that of LPCL, and it was enhanced with the increase in the relative DB of the HPCLs through the entire range of experimental temperatures. In addition, the apparent activation energy, E_a, was estimated from the curve fittings of the correlation times with the Arrhenius equation. The lower E_a was the result of the hyperbranched molecules, compared with that of their linear counterpart, and E_a of the HPCLs was observed to decrease with increasing relative DB, which indicates that the higher molecular mobility, and consequently, the easier molecular motion in the HPCL molecules were endowed with the shorter intrinsic branches and with the increase in the relative DB.

Acknowledgment. We are grateful to the Ministry of Environment, Republic of Korea for their support of this study through the Eco-Technopia 21 project.

CM0487021